

Modelling of Carbon Black Loadings Effect on the Heat Capacity of SBR and BR

Mohammad Ali Semsarzadeh^{1*}, Ali Yavarnia¹, and
Gholam Reza Bakhshandeh²

(1) Polymer Group, Technical Engineering Faculty, Tarbiat Modarres University
P.O. Box: 14155/4838, Tehran, I.R. Iran

(2) Department of Rubber Engineering and Processing, Iran Polymer and
Petrochemical Institute, P.O. Box: 14965/115, Tehran, I.R. Iran

Received 24 February 2002; accepted 3 November 2004

ABSTRACT

Thermal and rheometric behaviours of SBR and BR are important in the curing of rubbers. In this study, thermal analysis is used to determine the effect of carbon black (CB) loadings on the reactivity of sulphur in curing reaction, rate constants and heat capacities of rubbers. The heat capacities of SBR and BR are modelled at different loadings of carbon black. This modelling is confirmed by the rheometric studies of carbon black loadings effects on the activation energy of the curing process at different temperatures. The allylic hydrogens of BR and SBR are used to explain the rate constants and activation energies of the curing reactions. A semi-empirical relation is developed for heat capacities of SBR and BR rubbers containing carbon black.

Key Words:

heat capacity;
carbon black;
curing;
rate constant;
activation energy.

INTRODUCTION

The tyre manufacturing greatly depends on thermal behaviour of rubber and its vulcanization. Since chemical structure, molecular weight, and cross-link density and distribution can greatly influence the physical properties and stability of

rubber; they are important in the optimization process of vulcanization [1-3]. Although the rate of vulcanization increases with temperature, but the dissociation of sulphur bonds in rubber strongly limits this process and makes it industrially unfavourable.

(*) To whom correspondence should be addressed.
E-mail: semsarzadeh@modares.ac.ir

Therefore, tyre manufacturers favour this control by the reactivities of sulphur and accelerator. Additional amounts of sulphur and accelerator can increase the rate of formation of monosulphide and disulphides that improve rubber stability, while the rate of formation of polysulphides can reduce its stability especially on aging.

Since the effect of CB on thermal and rheometric behaviours of SBR and BR is not clear [3-4], the behaviours of SBR and BR with different weight percents of carbon black are studied. The behaviour of rubber during the curing is also not known and it is difficult to determine the reactivity of sulphur, while thermal behaviour or more specifically the heat capacity of the process in the presence of CB is missing.

In this paper the rate constants and activation energies of the curing of SBR and BR are reported and a semi-empirical relation is developed to show the effect of CB loadings on the heat capacities of SBR and BR.

EXPERIMENTAL

Material and Equipment

SBR and BR were supplied by Iranian Petrochemicals (Bandar Emam and Arak). Zinc oxide (99.5% purity) was obtained from Ranginah Pars. Natural rubber, stearic acid (0.89 g/cm³), sulphur (1.6 g/cm³) and carbon black (CB) grade N330 were commercial grades. The rubber formulations were carried out according to ASTM D3189-85 for 6 min at 120-130°C in a banbury (77RPM).

The rubber samples were prepared from two-roll mill, at 120-130°C at 2 kg/cm² pressure; with 5 mm thickness. Rheometric measurements were carried out by Zwick Rheometer. Thermal analysis was carried out by STA 625 scanning thermal analyzer.

Thermodynamic Studies of Rubbers

Thermodynamic studies of rubber materials were carried out for selected formulations of rubber compounds with various amounts of CB shown in Table 1. An internal mixer was used to produce a homogeneously dispersed rubber material. In the curing process, the accelerator *N-t*-butyl-2-benzthiazol sulphenamide (TBBS) decomposes upon heating to produce -S and -N radicals. Zinc oxide and stearic acid activate sulphur to pro-

Table 1. BR and SBR rubber compounds.

Sample No.	BR	SBR	CB
1	—	100	20
2	—	100	40
3	—	100	60
4	—	100	80
5	100	—	20
6	100	—	40
7	100	—	60
8	100	—	80

duce -SX radicals.

Prior to the curing, rubber compounds were mixed with CB and oil, the presence of oil in the rubber formulation, make a colloidal system of dispersed phase of CB aggregates in the rubber [3,5].

The thermal and rheological studies of rubber depend on the mixing parameters of this process. Since the mixing must ultimately reduce the size of the aggregates and break them into smaller agglomerates; therefore, the powdering, tearing, stretching-pulling, adhesion, and twisting around the rotor took place. At this stage, the spherical shell are made up of the inner bound rubber, and an outer mobile phase with the CB aggregates forms a disperse phase of this colloidal state.

Thermodynamically, addition of oil may dissolve the polymer, therefore a high degree of dispersion and distribution of particles requires miscibility. The miscibility of SBR-BR and SBR-NR may be expressed by eqns (1-3) [6]:

$$\chi = \frac{(\delta_1 - \delta_2)^2 V_1}{RT} \quad (1)$$

$$\delta_1 = \left(\frac{E_1}{V_1}\right)^{1/2} \quad (2)$$

$$\chi \leq 0 \quad (3)$$

The difference in solubility (ΔS) of SBR-BR is less than 0.31, while this difference for SBR-NR is about 0.41. The interphase boundary layer and interfacial tension are also related to the solubility and reduced interfacial tension of the rubber according to eqn (4) [7]:

$$\gamma_{23} \sim \chi^{1/2} \sim [\delta_2 - \delta_3] \quad (4)$$

The same thermodynamic relation holds for the adhesion between rubber components and the interaction parameter (χ) is a determined factor in this process. The rheological properties of SBR-NR and EPDM-BR also support these findings [4,8]. During this process as CB disperses in the rubber, viscosity increases and the oil is adsorbed by it. As the mixing continues the CB particles are crushed. At this stage, the long polymer molecules are held together around CB, and shear stress on agglomerate surfaces exceed its cohesive strength and therefore it destroys the larger agglomerates of the solid particles.

Recently, a serious attempt has been made to use power law to model the degree of dispersion of solid particles in the rubber before curing. These results show that dispersion of CB particles depends on shear rate, stress, and the power consumption of the mixer. This process also depends on the rotor rotation, and its minimum distance from the chamber wall [3,5,8].

Although, the rheological studies show a non-isothermal process in which torque drops with the increasing temperature during the mixing, the kinetics of dispersion for uncured rubber is not clear. However, certain rheological and thermal experiments are presently used to calculate the rate of vulcanization, activation energy, and heat capacity of reactions involved in the mass transfer of sulphur and accelerator during the moulding.

In this study, it is assumed that diffusion of the cross-linking agents require penetration in all directions; but since the cross-linking agents distribute easier in one phase than the other, the miscibility determines phases involved according to eqns (6-8). These equations are used to show the average diffusion coefficient (D) of the accelerator with respect to time (t) and displacement (x) in the elastomer [9, 10].

$$x = (Dt)^{1/2} \quad (5)$$

$$D_{\text{TBBS}} = 10^{-1} - 10^{-8} \text{ cm}^2/\text{s} \quad (6)$$

Sulphur has higher solubility in SBR and BR than the accelerator, and its distribution coefficient is about 1.03; this shows that penetration and transportation of accelerator into the target phase takes place at shorter

time. This effect is important in the moulding process, where heat transfer from the mould by conduction and the width of the phase boundary are expected to be increased by sulphur diffusion. There has been little attempt to study the effect of CB on thermal and rheological behaviours of rubbers or on their heat balance during the vulcanization. Heat capacity (C_p) and exothermic enthalpy (ΔH) are related to the vulcanization of rubber according to eqn (7).

$$\rho C_p \frac{dT}{dt} = q + \frac{\partial}{\partial x} \left(\kappa \frac{\partial T}{\partial x} \right) \quad (7)$$

In this equation; κ and ρ are heat conductivity and density of rubber, respectively. Thermogravimetric, differential thermogravimetric (TG-DTG), and differential scanning calorimetric (DSC) studies of SBR and BR are used to show the effect of CB. Thermal analysis of rubbers are presented in Tables 2 and 3, and their Thermal behaviours are shown in Figures 1-6. The heat capacity of BR curing is shown in Figure 7. The heat produced during the curing or vulcanization is calculated from the differential thermal studies of rubber compounds at a given temperature, where the degree of curing or vulcanization (DV) is defined as [9]:

$$DV = \frac{Q(t_i)}{Q_\infty} \quad (8)$$

Table 2. Thermal analysis of rubber compounds: differential scanning calorimetry (DSC) and thermogravimetric analysis (TG) at 20°C/min heating rates under N₂.

Sample	Peak temperature (°C)	Weight loss (%)	Enthalpy (J/g)
NR	216.94	—	-1232.56
	449.15	89.725	-709.15
	598.82	98.958	—
SBR	186.97	—	-62.95
			-223.61
BR	417.69	87.941	-289.16
	179.09	—	-66.51
	334.62	—	-405.45
	530.39	92.366	—

In this equation $Q(t_i)$ is the heat produced up to time t_i , and Q_∞ is the total heat produced during the complete cycle of vulcanization. The heat produced (\dot{q}) in this

process is calculated according to eqn (9):

$$q_i = \frac{dQ(t_i)}{dt} = \dot{q} \tag{9}$$

Table 3. Thermal analysis of SBR, BR and NR.

Rubber	Temperature range (°C)	Weight loss (%)	Heat (kJ/kg)
SBR	186-418	5.50	285
	418-500	82.20	289
BR	180-290	—	66.50
	400-480	—	405
	400-500	92.30	—
NR	217-450	89	1230

The heat capacities of SBR and BR compounds are calculated from DSC results according to the polynomial eqn (10).

$$C_p = A + BT + CT^2 + DT^3 + ET^4 + FT^5 + GT^6 \tag{10}$$

The coefficients and C_p thermal range of SBR and BR compounds at minimum and maximum temperatures are shown in Tables 4 and 5. The rate of vulcanization by using $\alpha = H_p/\Delta H$, $\beta = (dT/dt)$, and $b = dT \cdot dt$ may be

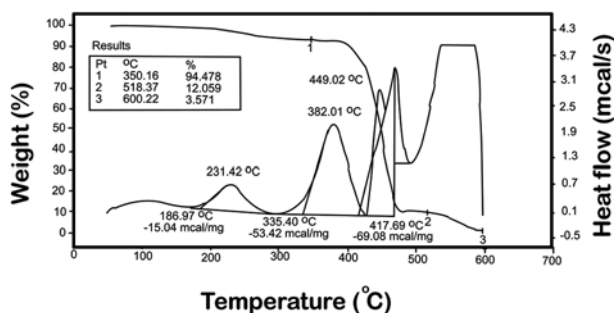


Figure 1. DSC and TG curves of SBR.

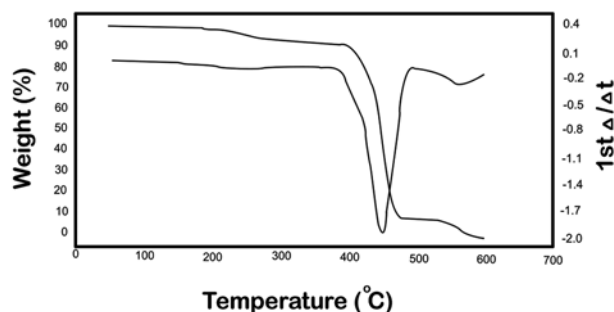


Figure 4. TG and DTG curves of SBR.

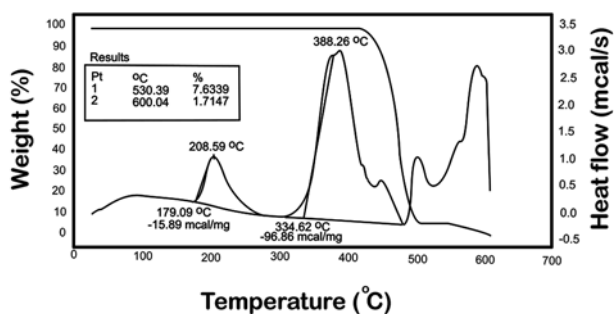


Figure 2. DSC and TG curves of BR.

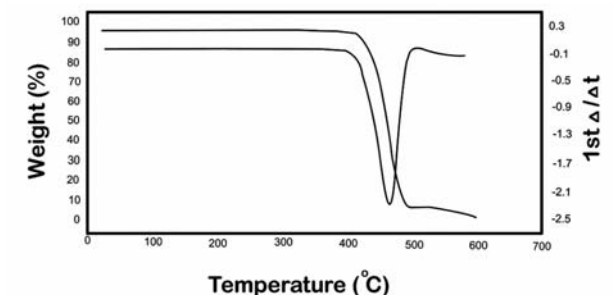


Figure 5. TG and DTG curves of BR.

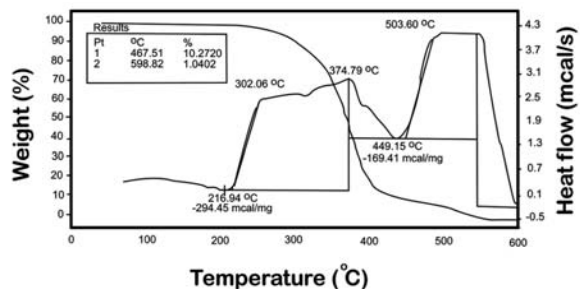


Figure 3. DSC and TG curves of NR.

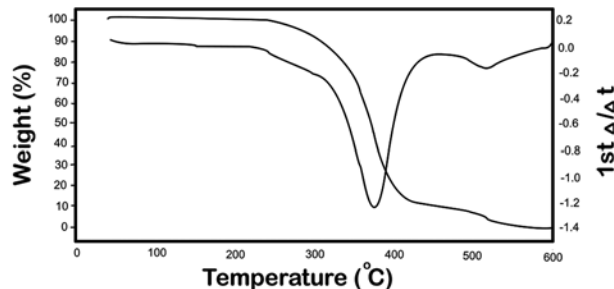


Figure 6. TG and DTG curves of NR.

Table 4. The polynomial coefficients of the heat capacity equations of SBR and BR formulation before curing at lower temperatures.

Sample No	Temperature range (°C)	A	B	C × 10 ³	D × 10 ⁶	E × 10 ⁹	F × 10 ¹¹	G × 10 ¹³	R ²
2	40.180	0.6862	-0.204	4	-4	9	3	-1	0.9958
3	30.180	-0.372	0.0545	-13	20	-100	40	-6	0.9977
4	32.180	0.551	0.0491	-1.1	10	-100	40	-6	0.9988
6	40.180	-1.22	0.107	-2.7	40	-300	100	-20	0.9964
8	30.180	-0.840	0.0796	2.1	30	-200	70	-10	0.9938

Table 5. The polynomial coefficients of the heat capacity equations of SBR and BR formulation before curing at higher temperatures.

Sample No	Temperature range (°C)	A	B	C × 10 ³	D × 10 ⁶	E × 10 ⁹	F × 10 ¹¹	G × 10 ¹³	R ²
2	180-250	3691.2	-103.76	1.21	-7.5	3	-5	4	0.9991
3	180-250	3002	-85.25	1.005	-6.3	2	-4	3	0.9989
4	180-250	2311	-65.9	0.78	-4.9	2	-3	3	0.9994
6	180-250	7714	-216	2.5	-15.5	5	-20	8	0.9919
8	180-250	2757	-78.90	0.94	-59	2	-3	3	0.990
		-	-	-	-	-	-4	3	0.9967

written according to eqns (11)-(14).

$$\frac{d\alpha}{dt} = K(T)f[\alpha(t)h(\alpha, t)] \quad \begin{cases} h(\alpha, t) = 1 \\ f(\alpha) = (1 - \alpha)^n \end{cases} \quad (11)$$

$$\frac{d\alpha}{dt} = K_0 \exp\left(\frac{-E}{RT}\right)(1 - \alpha)^n \quad (12)$$

$$\ln\left(\frac{d\alpha}{dt}\right) = n[\ln(1 - \alpha)] + \ln K_0 - \frac{E}{RT} \quad (13)$$

$$\ln\left(\beta \frac{d\alpha}{dT}\right) = \ln K_0 - E/RT + n \ln(1 - \alpha) \quad (14)$$

Since ratio of $d\alpha/dT$ is constant, the activation energy of vulcanization is calculated from the slope of the heating rate, β , according to eqn (15).

$$\ln(\beta) = \ln K_0 - E/RT \quad (15)$$

The thermal analysis of pure rubber above 200°C is

shown in Table 3. Thermal behaviours of SBR, NR, and BR compounds show that more than 89% of rubber decomposes between 400-500°C. The exothermic enthalpy of NR is highest (1230 kJ/kg), and it is considerably higher than BR and SBR (405 and 289 kJ/kg). It is expected that, the statistically larger number of allylic hydrogens in NR compared to SBR and BR (7/3 and 3/4.0 ratios) are responsible for the higher reactivity of NR.

The exothermic behaviour of BR is shown in Figure 7 in form of heat capacity variations. The endothermic peak at 100-150°C is related to presence of oil and stearic acid in the rubber formulation. The

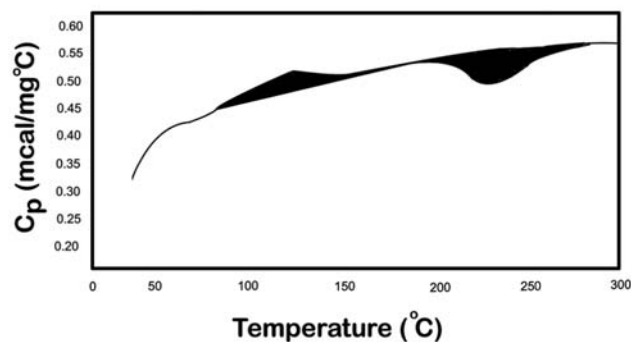
**Figure 7.** Heat capacity variation of BR in curing process.

Table 6. Thermal analysis of SBR and BR degradation.

No	Material	CB (phr)	Curing temperature (°C)			ΔH (J/g)
			338.25	389.36	472.00	
2	SBR	40	338.25	389.36	472.00	195.06
3	SBR	60	337.16	388.66	473.50	189.87
4	SBR	80	344.20	388.32	467.60	175.18
5	BR	40	339.63	365.63	467.60	288.45
7	BR	60	337.86	391.48	479.40	264.93

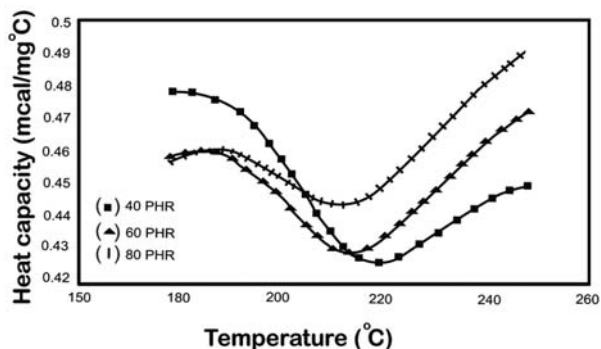
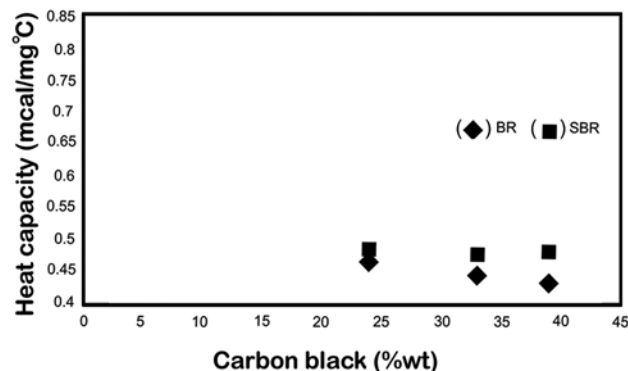
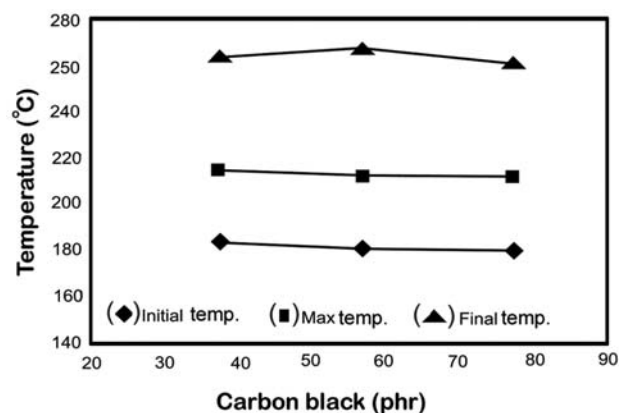
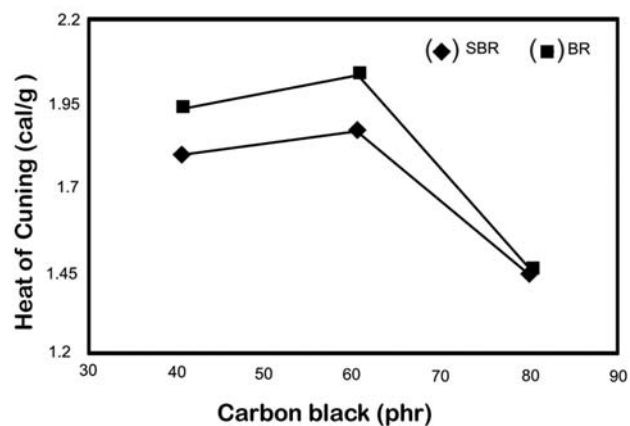
exothermic peak at 280-250°C is related to the curing of the rubber.

The effect of CB amount on the enthalpy of SBR and BR during the curing is shown in Tables 6 and 7. Since the enthalpy of curing depends on the heat transfer coefficient (h), the total area of sample (P), and the rate of heating (R), for SBR it is expected to shift the heat capacity or dH/dt to a lower temperature (eqns (16) and (17)):

$$\Delta H = h.P \quad (16)$$

$$\frac{dH}{dt} = \frac{dH}{dT} \cdot \frac{dT}{dt} = C_p.R \quad (17)$$

The recorded temperature and heat capacities of SBR and BR at different loadings of CB (40, 60, and 80 wt%) are shown in Figures 8 and 9, respectively. These effects on the curing temperature of SBR and heat of SBR and BR curing are shown in Figures 10 and 11, respectively. These results indicate that, the heat capacity of SBR with 40 wt% of CB is about 0.4 mcal/mg°C. In spite of the increased heat transfer of rubbers at high CB loadings (80 wt.%), Figure 11 shows that exothermic peaks are at their maximum in 60 wt.% of CB.

**Figure 8.** The effect of CB loadings on heat capacity of SBR.**Figure 9.** The effect of CB loadings on the heat capacity of SBR and BR.**Figure 10.** The effect of CB loadings on the curing temperature of SBR.**Figure 11.** The effect of CB loadings on the heat of curing of SBR and BR.

Although diffusions of sulphur and accelerator are fast, but transportations in three regions of CB-rubber (mobile, outer shell, and inner shell regions) are not the same and sulphur atoms cannot enter the same posi-

Table 7. Thermal analysis of SBR and BR during curing.

Sample No.	Material	CB (phr)	Curing temperature (°C)			ΔH (J/g)
			188.63	219.07	269.00	
2	SBR	40	188.63	219.07	269.00	7.28
3	SBR	60	185.56	216.82	272.00	7.61
4	SBR	80	184.18	216.06	265.00	5.86
5	BR	40	190.39	217.94	270.50	7.86
6	BR	60	186.67	217.89	262.61	8.33
7	BR	80	184.65	214.95	260.00	5.90

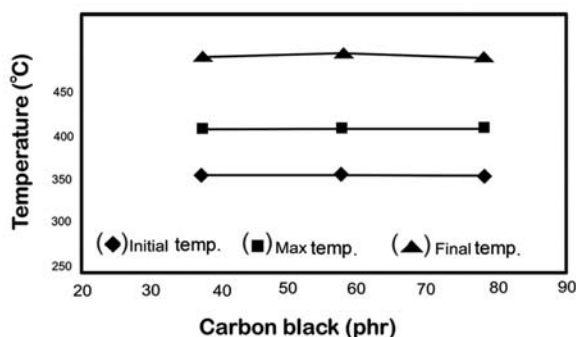
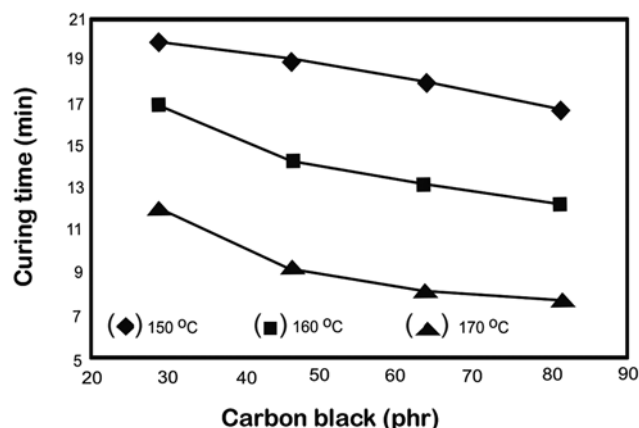
tions that are already occupied by CBs. The cross-linking agent also shows different miscibilities and interfacial tensions in three regions of CB-rubber which explains the reason of the dropping in enthalpies specially at the higher loadings of CB. But, at higher temperatures (340-467°C) decomposition reactions take place also and CB amount shows no effect on degradation of SBR (Figure 12). The higher loading of CB as is shown in Figure 13, reduces the curing time of SBR. Figure 14 shows that CB loadings have no significant effects on rate constants at 150°C and 160°C.

Rheometry of Rubber

The rate constant of vulcanization is estimated by a rheometer. Minimum and maximum torques (M_l and M_h) involved in the cured rubber compounds at a given temperature (150-170°C) are calculated from eqn (18):

$$\ln \left[\frac{M_h - M_l}{M_h - M_t} \right] = kt \quad (18)$$

In this equation M_t is the torque at 45% change. In spite of these advances, it is not yet clear how heat capacity

**Figure 12.** The effect of CB on the degradation temperature of SBR.**Figure 13.** The effect of CB on the curing time of SBR at 150, 160, and 170°C.

and activation energies change during the vulcanization in the mould. Certain equations are needed to model the heat capacity and heat generated during the vulcanization at different CB loadings or curing temperatures.

Rheometric studies are used to measure directly the viscosity of the rubber according to eqns (19) and (20) [12]:

$$M = \eta \Omega / k \quad (19)$$

$$\eta = 3M\theta_0 / 2\pi\Omega R^3 \quad (20)$$

where M , η , k , Ω , θ_0 , and R are torque, sample viscosity, instrument constant, rotational speed, cone angle ($\sim 3^\circ$) and radius, respectively. Rheometric curves of SBR and BR with different CB loadings at 150, 160, and 170°C are shown in Figures 15-16.

If curing of rubber is considered as first order reac-

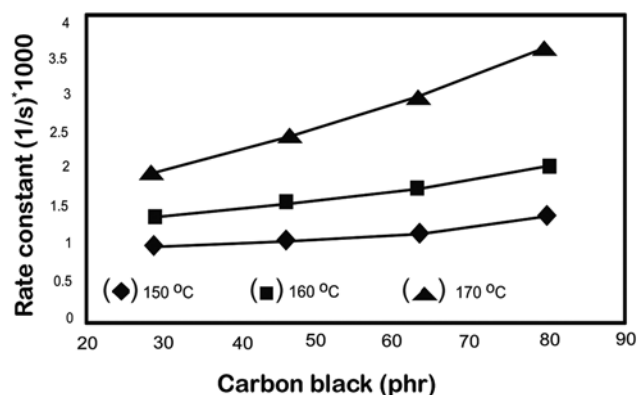
**Figure 14.** The effect of CB on the rate constant of curing reaction of SBR at 150, 160, and 170°C.

Table 8. The effect of carbon black and reaction time on the rate constant and activation energy of the curing of SBR and BR.

Sample No.	Temperature range (°C)	CB (phr)	Curing temperature (°C)			Rate constant ($k \times 10^3 s^{-1}$)			Activation energy (kJ/mol)
						150°C	160°C	170°C	
						1	SBR	20	
2	SBR	40	18.10	13.30	8.30	0.784	1.277	2.18	71.54
3	SBR	60	17.10	12.30	7.30	0.872	1.453	2.685	89.87
4	BR	80	15.80	11.40	6.90	1.056	1.74	3.320	91.18
5	BR	60	16.40	13.20	7.80	0.872	1.245	2.113	70.54

tion, its cross-linking density during the curing follows eqn (18). The measured torque at time t (M_t) and its

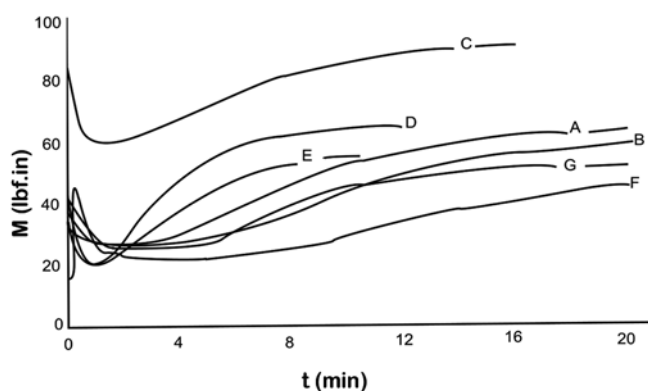


Figure 15. Rheometric behaviour of SBR with A : 60 phr CB at 160°C; B: 80 phr CB at 150°C; C: 80 phr CB at 160°C; D: 80 phr CB at 170°C; E: 60 phr CB at 150°C; and BR with F: 60 phr CB at 170°C; G: 40 phr CB at 150°C.

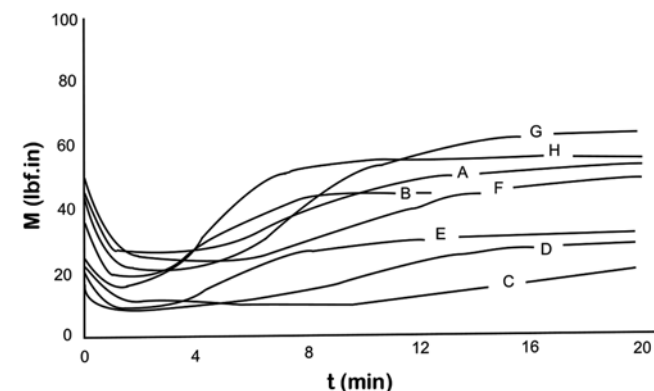


Figure 16. Rheometric behaviour of SBR with A : 40 phr CB at 160°C; B: 40 phr CB at 170°C; C: 20 phr CB at 150°C; D: 20 phr CB at 160°C; E: 20 phr CB at 170°C; and BR with F: 60 phr CB at 150°C; G: 60 phr CB at 160°C; H: 60 phr CB at 170°C.

minimum (M_t) were used to calculate the rate constant of curing at 150, 160, and 170°C.

The effect of CB on the curing time, temperature, rate constant (k), and activation energy (E_a) are shown in Table 8. Since curing rate depends on temperature and CB; the higher loading of CB increases the heat transferring to the activated accelerator complex, and facilitates the formation of higher order complexes with sulphur. At a higher temperature, additional polysulphide bonds not only increase the curing rate as

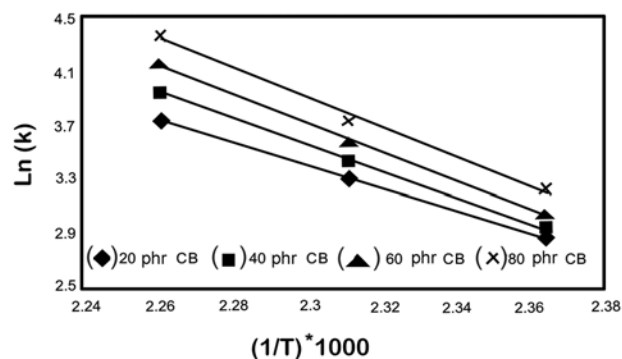


Figure 17. The effect of carbon black on the rheometric rate of curing of SBR.

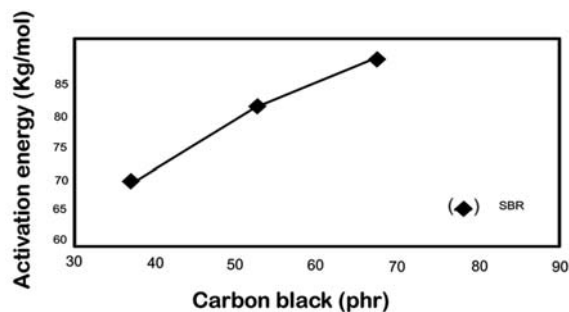


Figure 18. The effect of carbon black on the activation energy of the curing of SBR.

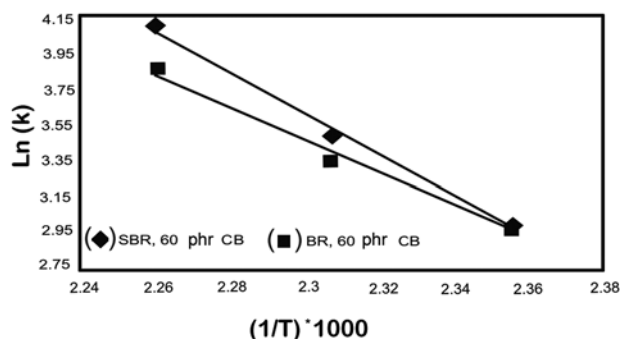


Figure 19. The effect of carbon black (60 phr) on the rate of curing of SBR and BR.

shown in Figure 17, but also increase its side reactions.

The energy of activation (E_a) for this process is calculated from eqn (15). The same results were derived from the slope of $\ln K$ vs. $1/T$ of the DSC curves. Since the activation energy of SBR is expected to remain constant at 91 kcal/mol (Figure 18) the possibility of side reactions are less at this temperature ($\sim 150^\circ\text{C}$). But at higher loadings of CB, the enthalpy is at its curing peak, and due to the statistically close numbers of allylic hydrogens for SBR and BR (3.3 and 4.0, respectively) it is expected to show the same rate of curing as shown in Figure 19.

Modelling of Heat Capacity

If we consider a statistically homogeneous field, based on the micro-heterogeneity of the material (MHM) and its bulk representative element (BRE) which fills it completely, then the effective property of the system such as heat conductivity or specific heat capacity may be defined accordingly. If the temperature on the surface is $T(s)$ and temperature gradient is ∇T ; then the heat flux q averaged over the volume V is expressed by eqn (21):

$$\bar{q} = -\kappa \nabla T \quad (21)$$

For the local regions of MHM, r is the vector radius:

$$q(r) = -\kappa(r) \nabla T \quad (22)$$

From the micro-scale, (dispersed CB particles) to macro-scale, (sample dimension) and mini scale L (dimensions of BRE); the effective properties are presented according to eqn (23):

$$L_0 \ll \langle l \rangle \ll L \quad (23)$$

If we express thermal conductivity or heat capacity according to eqn (24):

$$C_p = C_{p1} \phi A_1 + C_{p2} (1-\phi) A_2 \quad (24)$$

and heat flux q is directed along the layers; with parameter A and temperature gradient is expressed as:

$$\nabla T_1 = \nabla T_2 = \nabla T \quad A_1 = A_2 = 1 \quad (25)$$

One may present this relation along the layers as:

$$\phi A_1 + (1-\phi) A_2 = 1 \quad (26)$$

But, if heat capacity becomes additive, this relation may be written according to eqn (27):

$$C_p = C_{p1} \phi C_{p2} (1-\phi) \quad (27)$$

Although, The simplicity of these equations are

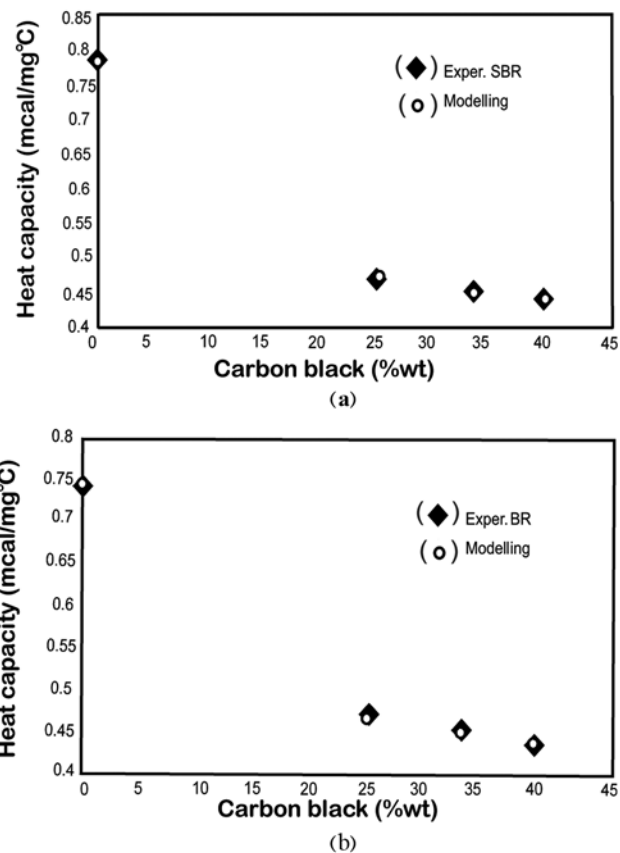


Figure 20. Modelling of heat capacity and CB in (a) SBR and (b) BR.

attractive, but they are not appropriate for modelling of rubber heat capacity and particle crowding or defects, thus it makes the modelling difficult. Another approach is to present these relations by a semi-empirical eqn (28).

$$\log C_p = \phi C_1 \log C_{p1} + (1-\phi) C_2 \log C_{p2} \quad (28)$$

This model which is shown in Figure 20 indicates that for the moderate loadings of CB, the heat capacities of SBR and BR fit best the results.

CONCLUSION

The thermal and rheometric analysis of the vulcanization reactions of SBR, and BR compounds are studied. The effect of CB loadings at different temperatures shows that activation energies of rubbers are the same at 60 phr of CB. Rheometric studies show that the rate constant depends on the reactivity of allylic hydrogens in SBR and BR. Thermodynamics of the curing depends on the CB loadings and heat transfer increases at higher loadings. A classical model is used to express the heat capacity of a single rubber formulation. A semi-empirical relation for the heat capacity of rubbers based on two different weight fractions of CB, seems to express this effect best.

ACKNOWLEDGEMENT

Authors wish to thank Iranian Institute of Polymer Research authorities for their cooperation and also Mr. M.G. Barvaz for his assistance in redrawing the Figures and make them ready for printing.

Nomenclatures

χ	Interaction-dimensionless
δ_1, δ_2	Solubility parameter of solvent, polymer, or two elastomers
E	Cohesion energy
γ_{23}	Surface tension
V	Molar volume of solvent cm^3/mol
D	Diffusion coefficient
t	Diffusion time, s

ρ	Density, g/cm^3
C_p	Heat capacity, kJ/mol
q	Heat of reaction, kJ
\dot{q}	Heat produced kJ/t
k	Thermal conductivity
dT/dt	Temperature gradient
n	Order of reaction
E	Activation energy, kJ/mol
T	Temperature, K
α	Extend reaction
β	Temperature gradient, or heating rate in DSC
d α /dt	Rate of vulcanization
H	Enthalpy, kJ/mol
M_h	Maximum torque, N/m^2
M_t	Torque at a given temperature, N/m^2
M_l	Minimum torque, N/m^2
η	Sample viscosity
k	Instrument constant
Ω	Rotational speed
θ	Core angle
R	Radius
\bar{q}	Average heat flux
ϕ	Volume fraction of elastomer

REFERENCES

1. Kauffman C.B., Seymour R.B., *Elastomers, J. Chem. Ed.*, **67**, 422-425 (1990).
2. Aksenov V.I., Afanaseva V.V., Sokolova A.D., Khlustikov V.I., Properties of blends of SKD polybutadiene rubber with high and low molecular weight 1,2-polybutadiene, *Int. Polym. Sci. Technol.*, **20**, 40-43 (1993).
3. Yoshida T., Fundamental theory of rubber mixing, *Int. Polym. Sci. Tech.*, **20**, 29-39 (1993).
4. Chough S.H., Chang D.H., Kinetics of sulfur vulcanization of NR, BR, SBR, and their blends using rheometer and DSC, *J. Appl. Polym. Sci.*, **61**, 449-454 (1996).
5. Yamalkin A., Baranov A.V., Blinov A.I., Modelling Non-isothermal mixing in rotor mixer, *Int. Polym. Proc.* **XV**, 115-121 (1999).
6. Pritykin L.M., Neikovskii S.I., Bolshakov V.I., New method for calculating the parameter of interaction in polymer blends, *Int. Polym. Sci., Tech.*, **23**, 95-97 (1996).
7. Schuster R.H., Relation between morphology of blends and physical properties of the elastomers, *Int. Polym. Sci. Tech.*, **24**, 5-13 (1997).

8. Go J.H., Ha C.S., Rheology and properties of EPDM/BR blends with or without a homogenizing agent or coupling agent, *J. Appl. Polym. Sci.*, **62**, 509-521 (1996).
9. Steen J., Aben W.J., Wapennar K.E., Optimization of vulcanization process of rubber products, *Polym. Eng. Sci.*, **33**, 183-189 (1993).
10. Nakauchi H., Inoue S., Naito K., Investigation of cross-link density and basic physical properties of rubber, *Int. Polym. Sci. Tech.*, **20**, 11-17 (1993).
11. Collyer A.A., Clegg D.W., *Rheological Measurement*, Chapman and Hall, London (1988).
12. Prevako V.A., Novikov V.V., *The Science of Heterogeneous Polymers*, John Wiley, New York (1995).